Effect of microtextured substrates on the molecular orientation of a nematic liquid-crystal sample

F. Batalioto,[1] I. H. Bechtold,[1] E. A. Oliveira,[1] and L. R. Evangelista[2]
[1]*Instituto de Física, Universidade de São Paulo P. O. Box 66318, São Paulo 05389-970, SP, Brazil*
[2]*Departamento de Física, Universidade Estadual de Maringá, Avenida Colombo, 5790, 87020-900 Maringá, Paraná, Brazil*
(Received 7 December 2004; revised manuscript received 21 June 2005; published 22 September 2005)

The in-plane orientation of a nematic liquid-crystal sample, confined by two periodic microtextured substrates, is theoretically analyzed by means of the Frank-Oseen continuum elastic theory and a suitable surface term. In addition, an easy optical method to produce such textures using photopolymeric films is presented. It is shown that, in the limit of large pattern period, the orientation depends only on the ratio of the splay and bend elastic constants K_1/K_3 and on the easy axis direction of the individual stripes. In the particular case for which $K_1=K_3$, the stability depends only on the easy axis direction for a general pattern period.

DOI: 10.1103/PhysRevE.72.031710 PACS number(s): 61.30.Hn, 61.30.Dk

Alignment of nematic liquid crystals (LCs) by spatially inhomogeneous surfaces has been analyzed since the pioneering work of Berreman [1], who investigated the anchoring effect of a periodically undulating surface, where the surface anchoring is locally strong. The influence of inhomogeneous surfaces on the molecular orientation of a LC sample has been analyzed by several authors in the framework of the Frank-Oseen elasticity [2–10]. Recently, a nanorubbing technique was applied on a polymer to produce orientational surface patterns with neighboring orthogonal square domains, leading to an in-plane surface bistability [11,12]. Subsequently, the same authors extended this symmetry approach to obtain a tristable nematic LC order [13]. The particular interest in patterned substrates and multistable devices is that they may allow the complete control of the LC orientation direction and the reduction of energy consumption during the optical activity [13,14].

In the previous works, the textured surfaces were produced by nanorubbing techniques, using an atomic force microscope stylus to create structures in the micrometer range. In this work, we present an easy method using optical techniques to produce microtextures and a theoretical analysis of the orientational conditions of a nematic LC sandwiched between two identical textured substrates. A schematic representation of this substrate can be seen in Fig. 1, where a pattern period L of the texture and the Cartesian coordinate system are shown. In this figure, the diagonal lines represent the easy axis directions made by the angle α with the x axis. We suppose a flat substrate, i.e., without any topographic variations.

The textures can be produced on azo-containing polymer films, for which the photoalignment of the azo groups is governed by the *trans-cis-trans* photoisomerization process [15]. An example of a periodic microtexture with $L=15$ μm and $\alpha \approx +60° \pm 3°$ and $-60° \pm 3°$ is shown in the optical image of the film in Fig. 2(a), obtained by a polarized microscope. The contrast in the figure arises from the different orientation induced to the azo groups on the individual stripes due to the uncertain of ±3°, seen between crossed polarizers. The polymer (PS 119®-Aldrich) was dissolved 0.2 wt.% in water and coated on a glass substrate by the casting method. The film was first homogeneously photoaligned at $\alpha=+60° \pm 3°$ using linear polarized light of a Nd:YAG laser ($\lambda=532$ nm). Then, a second irraditation is done by using the experimental setup illustrated in Fig. 2(b). The sample holder consists of a mirror with the plane fixed at 90 degrees from the place where the sample is positioned

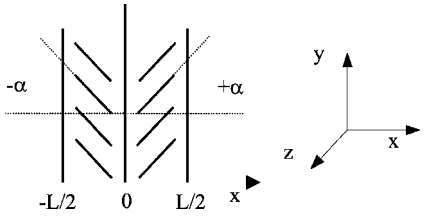

FIG. 1. Schematic representation of the pattern periodic microtextured substrate used in this work.

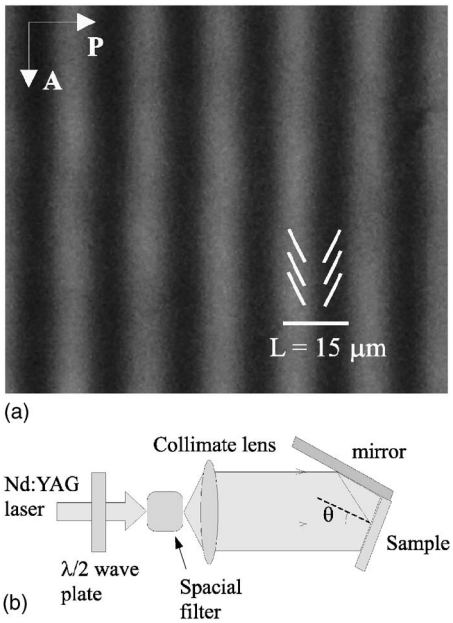

FIG. 2. (a) Microtexture of period $L=15$ μm inscribed on a photopolymer film with $\alpha \approx +60°$ and $-60°$; (b) experimental setup. The periodicity of the interference pattern is given by $L=\lambda/2 \sin \theta$.

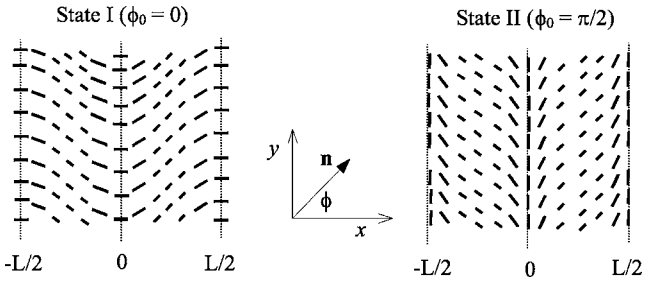

FIG. 3. Possible director configurations: state I, with $\phi_0=0$; state II, with $\phi_0=\pi/2$.

(which is the region where the interference fringes will be formed). This holder is mounted on a rotation stage, which enables the angle θ to be set according to the desired periodicity, given by $L=\lambda/2\sin\theta$ ($\theta=1^0\rightarrow L\approx 15$ μm). The polarization of incident light is rotated, in order to have the direction of photoalignment at $\alpha=-60°\pm3°$, in the illuminated regions, whereas the photoalignment direction remains unchanged in the dark regions. This technique allows the production of textures with periodicities down to the light wavelength, and α can be controlled using a $\lambda/2$ waveplate to set the incoming polarization direction. A complete description of this experimental method will be published elsewhere.

Let us consider a nematic LC sample of thickness d bounded at both sides ($z=0$ and $z=d$) by two identical patterned substrates exactly aligned, as described in Fig. 1. If the period L is much larger than the nematic correlation length, the LC director **n** tends to align parallel to the easy axis in each domain, with a continuous distortion through the borders of these domains. With these assumptions, it is expected that (i) the director **n** lies parallel to the xy plane and (ii) at the boundary of the domains, $x=nL/2$ ($n=0,\pm1,\pm2,\ldots$), the angle between the director and the x axis can be either $\phi_0=0$ or $\pi/2$, corresponding to the different states presented in Fig. 3. To calculate the preferred configuration of the system, we use the Frank-Oseen continuum elastic theory and a suitable surface term, which represents the surface LC interaction.

The total energy of the system is

$$F=\int d^3r[F_d(\mathbf{r})+F_S], \tag{1}$$

where

$$F_d(\mathbf{r})=\frac{1}{2}K_1(\boldsymbol{\nabla}\cdot\mathbf{n})^2+\frac{1}{2}K_3(\mathbf{n}\times\boldsymbol{\nabla}\times\mathbf{n})^2 \tag{2}$$

is the elastic energy density [16], where K_1 and K_3 are the splay and bend elastic constants, respectively, and

$$F_S=\frac{1}{2}W\sin^2[\phi(x)-\alpha]\delta(z) \tag{3}$$

is the frequently used Rapini-Papoular form for the anchoring energy [17], where Eq. (3) refers to both surfaces. In this equation $W=2W_S$, where W_S is the anchoring energy strength of each surface and $\delta(z)$ is the one-dimensional delta function. Since it is assumed that the two substrates are identical and exactly aligned, the director **n** lies parallel to the xy plane [18] and, therefore, the LC director **n** can be written as

$$\mathbf{n}=(\cos[\phi(x)],\sin[\phi(x)],0). \tag{4}$$

The resulting total energy F for the in-plane director **n** in our coordinate system can be written as

$$F=\int d^3r\frac{1}{2}\left\{K_1\sin^2[\phi(x)]\left[\frac{d\phi(x)}{dx}\right]^2+K_3\cos^2[\phi(x)]\times\left[\frac{d\phi(x)}{dx}\right]^2+W\sin^2[\phi(x)-\alpha]\delta(z)\right\}.$$

By integrating the above expression, the energy per unit area can be written as

$$\frac{F}{ld}=4\int_0^{L/4}\frac{1}{2}\left\{K_1\sin^2[\phi(x)]\left[\frac{d\phi(x)}{dx}\right]^2+K_3\cos^2[\phi(x)]\times\left[\frac{d\phi(x)}{dx}\right]^2+\left(\frac{W}{d}\right)\sin^2[\phi(x)-\alpha]\right\}dx, \tag{5}$$

where l is a length due to the integration in y, and d is the thickness of the sample, resulting from the integration in z. In the limit of large L, or when $K_1=K_3$, the energy per unit area can be obtained by integrating only from zero to $L/4$, instead of integrating on the whole period (from $-L/2$ to $L/2$). This can be done due to the symmetry of the system for large L, or when the elastic constants of splay and bend are the same ($K_1=K_3$). It means that the energies of the regions between $x=0$ and $x=L/4$ and between $x=L/4$ and $x=L/2$, for example, are the same. This is also valid for the surface energy term because its value remains the same by changing α to $\alpha+\pi$. To find the equilibrium profile of $\phi(x)$, one has to minimize the expression (5) by solving the Euler-Lagrange equation. After a first integration, the result is the following first-order differential equation:

$$\left[\frac{d\phi(x)}{dx}\right]^2=\frac{\left(\frac{W}{d}\right)\sin^2[\phi(x)-\alpha]-C}{K_1\sin^2[\phi(x)]+K_3\cos^2[\phi(x)]}, \tag{6}$$

where C is an integration constant. A general way to determine C is by applying Eq. (6) into Eq. (5), where the minimization of the resulting expression with respect to C can be performed numerically. In the limit of large L, however, one can easily determine the constant C by realizing that, in this limit, $\phi(x)=\alpha$ in the middle of the domains, i.e., in $x=n(L/2)+L/4$, and that

$$\left[\frac{d\phi(x)}{dx}\right]_{x=nL/2+L/4}=0. \tag{7}$$

From these conditions, it is possible to find that $C=0$ for large L (which means ≈50 μm or higher), and Eq. (6) is given by

$$\left[\frac{d\phi(x)}{dx}\right]^2=\left(\frac{W}{d}\right)\frac{\sin^2[\phi(x)-\alpha]}{K_1\sin^2[\phi(x)]+K_3\cos^2[\phi(x)]}. \tag{8}$$

For a general L, the condition (7) is also valid. However, in this case, $\phi(x)$ is different from α in the middle of the

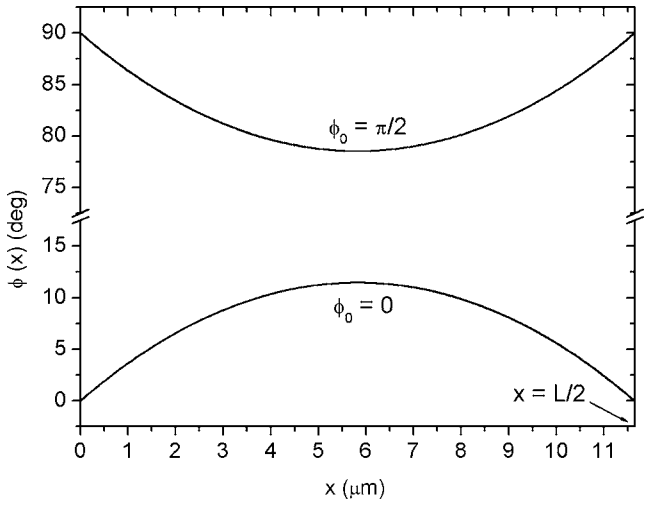

FIG. 4. An example of the profile $\phi(x)$ calculated from Eq. (6), for the two values of ϕ_0 at the border of the domain, $\phi_0=\pi/2$ and $\phi_0=0$.

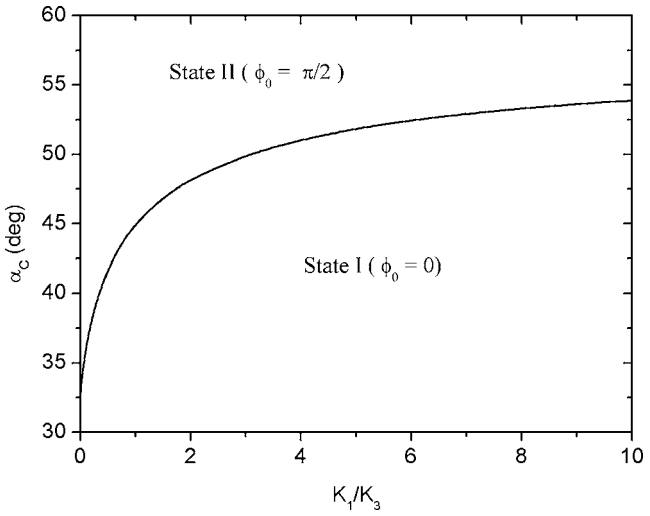

FIG. 5. The critical angle α_C as a function of the ratio of the splay and bend elastic constants K_1 and K_3 calculated from Eq. (8). The critical region is indicated by the solid line.

domains and also the constant C is not zero. An example of the $\phi(x)$ profile for a general pattern period L is shown in Fig. 4 for both values of ϕ_0 from $x=0$ to $x=L/2$. To make this figure, $\phi(x)$ was calculated from 0 to $L/4$ by using Eq. (6). As $K_1=K_3$, the result of $\phi(x)$ from $L/4$ to $L/2$ is symmetric to the one calculated for the interval 0 to $L/4$. We used the following parameters values: $W_S=2.5\times10^{-6}$ J/m^2, $d=20$ μm, $\alpha=45°$, and $K_1=K_3=10^{-11}$ N.

From Eq. (8) it is possible to determine which one of the two different configurations ($\phi_0=0$ or $\phi_0=\pi/2$) the system prefers to adopt, by comparing the total energy of these two configurations. Evidently, the preferred configuration depends on the angle α of the easy axis, however there exists an angle for which the energy is the same in both configurations. This is a critical angle that we call α_C. It means that, for a system with $\alpha=\alpha_C$, both states (I and II) are stable. For $\alpha<\alpha_C$, the system should prefer the configuration with $\phi_0=0$ in $x=nL/2$ (state I), whereas for $\alpha>\alpha_C$ the system prefers the configuration with $\phi_0=\pi/2$ (state II).

For a general pattern period L, the critical angle α_C depends on the specific values of the quantities W,d,K_1, and K_3, due to the constant C variation for different values of these parameters. In the limit of large L, however, $\phi(x=nL/2+L/4)$ is always equal to α, reflecting the fact that far from the domain boundaries the LC director should align parallel to the easy axis. As a consequence, the critical angle α_C is independent of all particular values of the anchoring energy strength W or the sample's thickness, d; it is also independent of the particular values of the elastic constants K_1 and K_3. In fact, according to our calculation, in the limit of large L, the critical angle α_C depends only on the ratio of the elastic constants K_1/K_3.

The calculation to find α_C was performed by looking for the value of α for which the energy F calculated with $\phi_0=0$ and with $\phi_0=\pi/2$ are the same. By using Eq. (8), we found that the critical angle is observed for $\alpha=32.5°$ ($K_1/K_3\to0$) and $\alpha=57.5°$ ($K_1/K_3\to\infty$). The dependence of α_C as a function of the ratio K_1/K_3 is shown in Fig. 5 for $0<K_1/K_3<10$, where the solid line describes the situation in which both states I and II are equally probable, in the limit of large L. For example, by considering the LC 5CB (4-pentyl-4′-cyanobiphenyl) for which the value of $K_1/K_3=0.7$ [19], the critical point occurs at $\alpha_C=43.25°$. For any value of α below or above $\alpha_C=43.25°$, the LC director assumes a stable configuration in state I or state II, respectively. For this particular case, a stable configuration of the sample could be induced to state I or state II just by applying an in-plane electric field parallel to the x axis or y axis, respectively. By changing the value of α to lower or higher values, this condition of stability for both states is lost. Another example is given in Fig. 6, where the energy per unit area [Eq. (5)] is shown as a function of ϕ_0 for $K_1=K_3$, considering large L. As $K_1=K_3$, it is expected that $\alpha_C=45°$ (see Fig. 5). Actually, for $\alpha=45°$ two minima of the energy are observed at $\phi_0=0$ and $\phi_0=\pi/2$, and they have the same value. For $\alpha=30°$, i.e., $\alpha<\alpha_C$, the minimum of the energy

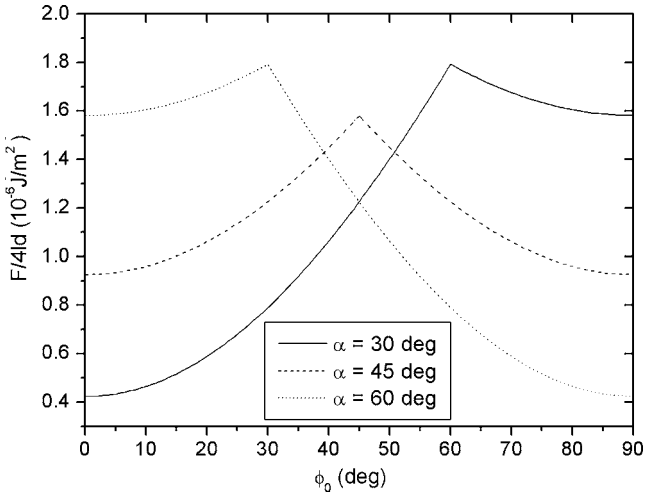

FIG. 6. The energy per unit area $F/(4ld)$ as a function of the angle at the domain boundaries ϕ_0 for $\alpha=30°$, 45°, and 60°.

per unit area occurs for $\phi_0=0$, showing that state I is the stable one. Finally, for $\alpha=60°$, i.e., $\alpha>\alpha_C$, the minimum is verified for $\phi_0=\pi/2$, indicating that state II is the stable state. This calculation was performed using Eq. (8) and the parameters values $K_1=K_3=10^{-11}$ N, $W_S=2.5\times10^{-6}$ J/m^2, $d=20$ μm, and $L=120$ μm.

It is well known that most of the nematic LCs show $K_3>K_1$; it means that the large region for which $K_1/K_3>1$, in Fig. 5, does not present a practical interest, but in our theoretical analysis it is important to observe the convergence limits. It is also important to emphasize that the value of K_1/K_3 is temperature-dependent. Therefore, the transitions between the two states can be temperature-induced.

When the pattern periodicity becomes small ($L\rightarrow0$), in such a manner that the director is no longer able to follow the orientation imposed by the easy axis in each domain, a homogeneous state of alignment is expected with $\phi_0=0$ or $\phi_0=\pi/2$. Therefore, the continuous decreasing of L, starting from any of the two stable states (I or II), would allow one to observe in-plane and out-of-plane orientational transitions. Experiments are in progress to detect these transitions. Such transitions have previously been reported by other authors for different systems [11,14,20,21].

In conclusion, we have analyzed the configuration of a nematic LC in contact with a microtextured patterned surface of period L along the x axis. The easy-axis direction in each domain makes alternating angles α and $-\alpha$ with the x axis. In the limit of large L, we have considered that the director is submitted to a continuous distortion and the orientation in the boundary of the domains can be either parallel or perpendicular to the x axis. The two possible configurations correspond to stable orientational states, called state I and state II. We have found that, depending on value of the ratio K_1/K_3, the two states are separated by a line (corresponding to α_C), where the two states present the same probability of occurring.

The authors are grateful to Professor G. Barbero for useful discussions and to CNPq and FAPESP for financial support.

[1] W. Berreman, Phys. Rev. Lett. **28**, 1683 (1972).
[2] M. Kléman, *Points, Lignes, Parois* (Editions de Physique, Les Ulis, Orsay, 1977).
[3] G. Barbero, Lett. Nuovo Cimento Soc. Ital. Fis., **29**, 553 (1980).
[4] G. Barbero, Lett. Nuovo Cimento Soc. Ital. Fis., **32**, 60 (1981).
[5] H. L. Ong, A. J. Hurd, and R. B. Meyer, J. Appl. Phys. **57**, 186 (1985).
[6] F. Lonberg and R. B. Meyer, Phys. Rev. Lett. **55**, 718 (1985).
[7] S. Faetti, Phys. Rev. A **36**, 408 (1987).
[8] G. Barbero, T. Beica, A. L. Alexe-Ionescu, and R. Moldovan, J. Phys. II **2**, 2011 (1992).
[9] L. R. Evangelista and G. Barbero, Phys. Rev. E **48**, 1163 (1993).
[10] L. R. Evangelista and G. Barbero, Phys. Rev. E **50**, 2120 (1994).
[11] J. H. Kim, M. Yoneya, J. Yamamoto, and H. Yokoyama, Appl. Phys. Lett. **78**, 3055 (2001).
[12] J. H. Kim, M. Yoneya, J. Yamamoto, and H. Yokoyama, Mol. Cryst. Liq. Cryst. Sci. Technol., Sect. A **367**, 151 (2001).
[13] J. H. Kim, M. Yoneya, and H. Yokoyama, Nature **420**, 159 (2002).
[14] B. Lee and N. Clark, Science **291**, 2576 (2001).
[15] A. Dhanabalan, C. R. Mendonça, D. T. Balogh, L. Misoguti, C. J. L. Constantino, J. A. Giacometti, S. C. Zilio, and O. N. Oliveira, Jr., Macromolecules **32**, 5277 (1999).
[16] C. W. Oseen, Trans. Faraday Soc. **29**, 883 (1933);F. C. Frank, Discuss. Faraday Soc. **25**, 19 (1958).
[17] A. Rapini and M. Papoular, J. Phys. (Paris), Colloq. **30**, C4-54 (1969).
[18] L. T. Thieghi, R. Barberi, J. J. Bonvent, E. A. Oliveira, J. A. Giacometti, and D. T. Balogh, Phys. Rev. E **67**, 041701 (2003).
[19] J. D. Bunning, T. E. Faber, and P. L. Sherrell, J. Phys. (Paris) **42**, 1175 (1981).
[20] B. Zhang, F. K. Lee, O. K. C. Tsui, and P. Sheng, Phys. Rev. Lett. **91**, 215501 (2003).
[21] O. K. C. Tsui, F. K. Lee, B. Zhang, and P. Sheng, Phys. Rev. E **69**, 021704 (2004).